Sādhanā (2021) 46:134
https://doi.org/10.1007/s12046-021-01661-w

Wear and corrosion characterisation of AISI 1030, AISI 1040 and AISI 1050 steel coated with Shielded Metal Arc Welding (SMAW) and Plasma Transfer Arc (PTA) methods

MUSTAFA ÖZGÜR ÖTEYAKA[1], ASLI ERGENEKON ARSLAN[2] and FATIH HAYATI ÇAKIR[1,*]

[1]Eskişehir Vocational School, Eskişehir Osmangazi Üniversitesi, Eskişehir, Turkey
[2]Vocational School, Bilecik Bilecik Şeyh Edebali Üniversitesi, Bilecik, Turkey
e-mail: moteyaka@ogu.edu.tr; asli.arslan@bilecik.edu.tr; fcakir@ogu.edu.tr

MS received 12 January 2021; revised 5 April 2021; accepted 10 June 2021

Abstract. In this study, the surface alloying process was carried out by using Plasma Transfer Arc (PTA) and Shielded Metal Arc Welding (SMAW) on the surfaces of plain carbon AISI 1030, 1040, 1050 steel materials. The performance of the coatings was evaluated by applying mechanical tests and electrochemical techniques. The results show that the resistance against the plastic deformation increased significantly by surface alloying; it reached the highest value of 896 HV with SMAW coating. The wear test findings exhibited that the surface alloying process improved the wear properties of the materials, and it was more pronounced for the coating powder Toolcord. In general, SiC+B_4C coated steels hard-faced with the PTA method demonstrated better corrosion potential and corrosion rate compared to SMAW coatings. This improvement is probably due to the attendance of boron oxide in the oxide film, making it more resistant against Cl^- attacks. The Nyquist analysis showed a semi-circle capacitive loop at high frequency and an inductive loop at low frequency for all samples. The electrochemical impedance spectroscopy analysis showed that better corrosion resistance was observed for 1030 when using PTA with powder SiC+B_4C, while for 1040 and 1050, it was SMAW with powder Citodur.

Keywords. Hard-facing; plain carbon steel; Plasma Transfer Arc (PTA); Shielded Metal Arc Welding (SMAW); wear; corrosion.

1. Introduction

In heavy industries, the parts were usually subjected to significant wear and corrosion degradation. Replacing every worn part is a high-cost solution. Hardfacing is a prominent technique that increases the durability or long-life service of heavy-duty parts. These methods allow companies to increase the service life of components, lower the total cost, and maximize their reliability and profit. Generally speaking, the surface of the substrate in this method is covered with a harder or near chemical composition material to substrate using different techniques with high energy input potential such as Plasma Transfer Arc (PTA), Tungsten Inert Gas (TIG), Shielded Metal Arc Welding (SMAW), etc. [1–5]. Among these methods, SMAW is the most preferred because of ease of use, low cost of the process, and because it makes it possible to obtain thick coating in a single pass. The purpose of this method is to provide a replacement for a worn surface with more special materials compared to traditionally used surfaces of the materials that are relatively low-cost to process and easy to find. Obtaining a hardface in the surface of the part is a lowe-cost solution comparing to using highly alloyed steels. Since the surface is the part where corrosion, wear, and fatigue generally initiates. There are many methods applied to generate surface alloying techniques; the most commonly used methods as energy sources are Tungsten Inert Gas, Plasma Transfer Arc, Laser Welding Carburization, nitrogen impregnated nitriding, or boron impregnated boronizing processes [6]. These methods are selected according to the base material used, and the aim is to form hard compounds at the surface of the material and generate a transition with the chemical and base material structure applied. The application of this method starts with selecting a powder that will be compatible with the substrate material, physically binding the selected powder to the area to be coated, or applying it during application [7, 8]. Several studies were conducted on the surface alloying by using SMAW and PTA to minimize the wear and corrosion degradation of steel parts. For example, Singh *et al* [1] conducted a study on the hardening of low steel carbon by using weld metal of AWS E7014 SMAW

*For correspondence
Published online: 06 July 2021

electrode with sodium silicate (binder) and chrome powders. It was found that applying lower current (110 A) and 90% of chrome powder reached a maximum hardness of 637 HV. The wear rate of the hard-faced sample increased with the increment of the current for all levels of chrome. Sadeghi *et al* [9] used gray cast iron as base metal and employed different electrodes for coatings such as Ni electrode (DIN8563), Carbon Steel electrode (DIN1913), and Hardening electrode (DIN8555) with SMAW technique. The wear test was performed to evaluate the performance of coatings. The results showed that all electrodes used in the study improved the wear resistance, and the Ni-based electrode blocked the formation of the martensitic phase. On the other hand, surface alloying with the PTA technique was investigated by different authors [10–13]. Ferozhkhan *et al* [10] deposited two layers of coatings, stainless steel (309-16L) and stellite 6, by flux-cored arc welding using ER309-16 electrode and PTA methods, respectively. The obtained hardness was reported as 600 $HV_{0.3}$ on the PTA surface, and the wear mechanism identified was delamination and abrasive wear. Ulutan *et al* [14] coated FeCrC composite on the AISI5115 steel rolling cylinder using PTA. The average coefficient of friction value was lower compared to the untreated substrate, and it varied between 0.62 and 0.73. Moreover, the lowest wear rate of 2.88×10^{-6} $mm^3/N/m$ was recorded after applying FeCrC coating at 100 Ampers.

The corrosion of steel in the atmosphere was very well studied in literature [15]. However, the corrosion performance and mechanism in marine corrosion of steel were not well established. Some works suggested that localized corrosion is often encountered in chloride media [16]. This behavior was directly related to the microstructure propriety of steel. It is well documented that pitting corrosion of steel was due to such surface defects as grain boundaries and inclusions. Especially the effects of surface alloying on corrosion resistance are not investigated thoroughly. Since the wearing of parts includes both mechanical and chemical aspects, electrochemical tests are required. The coating or assembly of steel parts by welding techniques is useful to join two parts or repair. The newly formed microstructure had an effect straight on the corrosion behavior of steel. Some studies were conducted on steel substrates by using SMAW [17–19]. For example, Srinivasan *et al* [18] showed that the E2209 electrode was better to use during joining duplex stainless steel and carbon steel against pitting corrosion in 1 M NaCl solution. On the other hand, the corrosion behavior of Cr-Mn stainless steel welded by SMAW (filler 308L-16) and TIG (filler 308 L) was examined by Bansod and Patil [19]. They found that the base metal was more active than SMAW and TIG-coated surfaces, respectively. The high resistance against corrosion of TIG samples was obtained due to a high proportion of delta ferrite in the weld zone. Moreover, they cited that the pitting resistance increase for TIG due to a higher quantity of δ -ferrite phase. It was reported by Busari *et al* [17] that high voltage and 135A during SMAW increased the corrosion resistance due to the formation of small grain size in the structure. The investigation of Mohammed *et al* [20] on arc-welded high nitrogen stainless steel in 3.5% NaCl solution showed that the coarse austenite grains with a lower quantity of δ-ferrite reduced galvanic activity in the weld zone. The effect of PTA with $SiC+B_4C$ powder on the corrosion of medium steel was not investigated previously to the best of our knowledge. However, different steels were investigated, such as duplex steel [21], AISI 304 stainless steel [22], and Hardox 400 steel [23]. For instance, the corrosion resistance of API 5L X70 steel used in pipeline manufacturing was coated using PTA with filler Nickel alloy AWS ER NiCrMo-3 (Inconel 625) [24]. The findings showed that sample 2, with a higher level of dilution and iron content, demonstrated lower E_{corr} (−0.343 V), but the I_{corr} was higher compared to sample 7 having lower dilution in the corrosive medium containing 60 ml of 0.1 M NaCl.

Plain carbon steel is a low-cost and well-known material that is used in general machine parts where wear and corrosion damage are predominant. The components, in general, have so far been coated using welds to increase their lifetime and against damage specified above. The goal of this work is to enhance the wear and corrosion resistance of mild steel using PTA and SMAW techniques to form a coating on the sample surface. The literature survey above showed that PTA coating using $SiC+B_4C$ powder was not investigated on the wear and corrosion performance of AISI 1030, AISI 1040, and AISI 1050. Moreover, the present study explores the SMAW method using a different filler such as Citodur 600 and Toolcord on the wear and corrosion performance of the plain steel and compares them to generated PTA coating.

2. Material and method

2.1 *Sample preparation*

In this study, AISI 1030, 1040, and 1050 alloys were selected as substrate materials. These alloys are plain carbon steels with different carbon amounts, which were supplied as rolled plates with 10 mm thickness. In order to adhere the powders to the substrate, a grove was machined using milling methods having a radius of 2.5 mm on the surface of the materials, as presented in figure 1. The coatings powders used were $SiC+B_4C$, Citodur 600, and Toolcord. The chemical compositions of the substrate and powders were given in table 1. The first coating powder contains a mixture of 50 wt.% SiC and 50 wt.% B_4C powders. The second coating powder contains a significant amount of Cr and Fe, and the third coating powder contains W, Mo, and Cr. In this study, a total of twelve specimens were prepared; three samples AISI 1030, 1040, 1050 were tested as the supplied state, and nine samples were tested

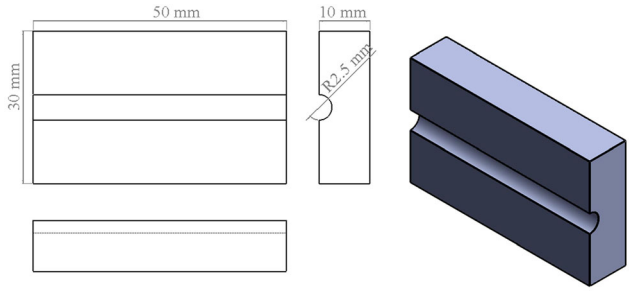

Figure 1. The technical drawing of the sample with groove open.

with different coatings on each of the three plain carbon steel surfaces. The procedures applied to the samples and the designation of the groups are given in table 2.

The purpose of selecting the base materials from plain carbon steels with different carbon amounts is to reveal the effects of the carbon amount on the success of the surface alloying procedure. Three different surface alloying processes were carried out on three different base materials. The methods followed for the coating have been selected and applied from among the methods in which the chosen powders can be applied successfully. PTA method was chosen to use the SiC+B_4C powder. The reason for this choice is the high energy input of this method makes it possible to apply different powders in many alloys [25]. Citodur 600 and Toolcord are commercial hard-facing electrodes. The coating process of these electrodes was employed with the method and parameters suggested by the supplier.

Before the surface alloying process, the plates were cut with a saw blade at the dimensions of 30 mm in width and 50 mm in length. In order to hold the coating powders in place, a radial groove with a 2.5 mm depth was milled. Powders were adhered to this groove by mixing with alcohol. The alcohol was used as a binder. The alcohol was blown off with an initial heating at 100°C. The coating process parameters were given in table 3.

Since the high energy input generates wavy surfaces, the surface of the samples was machined to obtain a ground surface. In machining, the grinding method was chosen to get a plain surface and to eliminate the risk of tool breakage. After machining, samples were cut with SiC precision cutting disc at dimensions approximately 10*10 mm from the middle part of the alloyed samples. The wear and corrosion tests were performed at the top of alloyed samples. The alloyed surface was then smoothed further by using abrasive sandpapers. The test samples were prepared by following steps for wear test; first, they were hot-molded at the temperature of 180°C for 3 minutes, then the molded samples were ground with 220 and 600 grid magnetic emery paper using Struers Tegraforce pneumatic grinding and polishing by applying water on the surface and 15 N load for 10 minutes. At the last stage, the polishing process was performed with similar apparatus. For this purpose, 3 μm diamond solution and appropriate polishing clothes were selected. At the end of metallographic preparation, the surface roughness of the samples was between 0.015 and 0.03 μm. Then, the prepared surface was cleaned with alcohol before wear tests.

2.2 *Hardness measurement and wear tests*

Hardness is an indication of the resistance of the samples to plastic deformation. Hardness testing is one of the most practical methods to evaluate the thickness and the effects of hardfaced coating. Since the hardness differences could change within small sections, it was decided to use a microhardness measurement method to observe these changes. For these tests, samples were cut axially from the face of the sample surface. In microhardness measurement, a Diamond Pyramid with an angle of 136° was used; the applied load was 100 grams force, and the dwell time was 10 seconds.

The wear performance of the sample was tested by a ball-on-disk test. Generally speaking, in the literature, two methods are preferred to evaluate the performance of surface coated alloys. One of these methods is abrasive testing, and the other one is adhesive testing. In this study, the adhesive testing method with a ball-on-disk wear configuration was selected. figure 2 shows a schematic representation of the wear test set-up. The wear tests were conducted without lubrication and at room temperature.

The wear tests were carried out according to the DIN 50324 standard. The CSM Tribometer equipment was used

Table 1. Chemical composition of the substrate and powders materials of surface alloying.

Element Weight%	Fe	C	Si	Mn	Cr	Mo	V	B	W
AISI 1030	Balance	0.270–0.340		0.60–0.90					
AISI 1040	Balance	0.370–0.440		0.60–0.90					
AISI 1050	Balance	0.470–0.55		0.60–0.90					
SiC+ B_4C		59.15	13.825					27.02	
Citodur 600	Balance	0.4	0.5	0,3	7	0.5	0.5	–	–
Toolcord	Balance	1.0	1.0	1.3	4.9	7.6	2.3	–	1.9

Table 2. Sample designation applied coating method and powder.

Sample Code	Base Material	Coating Method	Coating Powder
1030	AISI 1030	–	–
1040	AISI 1040	–	–
1050	AISI 1050	–	–
S1	AISI 1030	PTA	SiC+B_4C
S2	AISI 1040	PTA	SiC+B_4C
S3	AISI 1050	PTA	SiC+B_4C
S4	AISI 1030	SMAW	Citodur 600
S5	AISI 1040	SMAW	Citodur 600
S6	AISI 1050	SMAW	Citodur 600
S7	AISI 1030	SMAW	Toolcord
S8	AISI 1040	SMAW	Toolcord
S9	AISI 1050	SMAW	Toolcord

Table 3. Process parameters of the welding methods used for surface alloying.

Method	PTA	SMAW
Current (A)/Voltage (V)	150/20	120/15
Production speed (mm/s)	2.2	17
Electrode Diameter (mm)	4.6	3.25
Shielding Gas Flow Rate, Ar (l/min.)	15	–
Plasma Gas Flow Rate, Ar (l/min.)	0.2	–

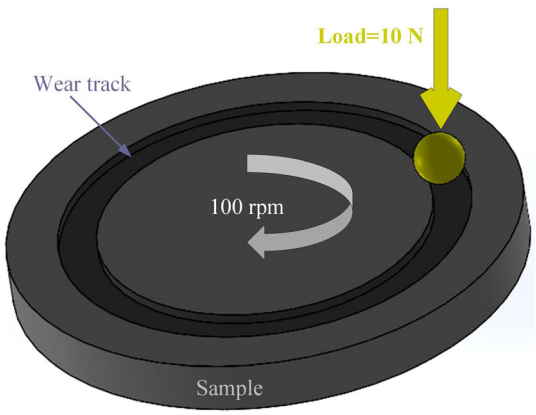

Figure 2. Schematic representation of wear test and wear test conditions.

with the counterpart WC-6% ball with a diameter of 3 mm. The selected ball had a hardness of 91.6 HRA with a modulus of elasticity of 690 GPa as given by the supplier. The coefficient of friction (COF) of each sample was found by applying wear parameters of 10 N load, 2.5 mm wear radius and distance of 50 m. At the end of the adhesive test, the worn area of the wear section was measured by using profilometer Mitutoyo SJ-401. The OriginLab-Demo software was employed to calculate the worn sections, and the worn area versus samples was graphically presented as results.

2.3 *Corrosion tests*

In order to conduct corrosion tests, the samples were cold-molded with a copper cable for obtaining an electrical connection between the sample to procure conductivity. The electrochemical tests were performed using a Gamry Interface 1000 potentiostat with a standard three-electrode cell system, working electrode (samples), reference electrode (standard silver chloride electrode), and counter electrode (graphite rod). The Gamry Echem Analyst software was conducted to analyze the data. The conductivity of the working electrode was achieved by copper wire using copper tape; then, they were firmly fixed with cold epoxy resin. To simulate the corrosive environment, a solution of 1 L of 3.5 wt.% NaCl was prepared from distilled water. The corrosion tests were begun after 15 min. of immersion of the working electrode (1 cm^2). The tests were repeated at least three times for each experimental condition. The passivation behavior of samples was investigated using the potentiodynamic polarization test; the experiments were conducted between −2 V and +2 V at a scan rate of 1 mV/s. The kinetic acts between the electrode surfaces and solutions were analyzed using electrochemical impedance spectroscopy (EIS). The Nyquist plots were recorded for each sample at potentiostatic mode with a frequency range of 100 kHz to 0.01 Hz at an amplitude of 10 mV.

3. Results and Discussion

3.1 *Hardness and wear behavior of coatings*

Microhardness measurement was made at vertical direction 100 μm intervals from the surface to the inside of the

sample. The results of measurements point out that the increase of hardness is the result of the presence of hard phases on the surface. High surface hardness may indicate that more resistant surfaces are obtained against wear and scratches. The hardness profile of untreated and coated samples was presented in figure 3. At first look, all the untreated samples had a similar average hardness ranging between 170–230 HV. The increasing carbon content increased hardness, but since all samples are testes as supplied state, which is a pearlitic state, the hardness difference among samples is limited. After coating with SiC + B_4C powder, a significant increase of hardness was observed, and an average of 400 HV was obtained for S1, S2, and S3 groups. This result was lower compared to the work of Ferozhkhan *et al* [10], where they measured 600 HV on the surface of stellite 6 coated on stainless steel using PTA. This possible lower value can be interpreted by the elastic behavior of the Si element, which softened the material. The plain carbon steel does not have additional alloying elements such as Cr or Mo, which could form carbides. The lack of alloying elements of plain carbon steel limited the obtained hardness comparing to Ferozhkhan's work. On the other hand, the electrode Citodur 600 increased the hardness to ∼ 500 HV for the groups S4, S5, and S6. Despite the Mo element, which helps ferrite formation (softening materials), carbide forming elements such as Cr and V increased the hardness of Citodur 600. Otherwise, the hard-faced samples of S7, S8, and S9 with Toolcord Electrode had the highest hardness of 896 HV compared to Citodur 600 Electrode and SiC+B_4C powder. This improved performance can be explained by the chemical composition of Toolcord, which involves W, Cr, and V. These elements probably support the formation of carbides and contribute to obtaining controlled cooling of the surface. Singh *et al* [1] also indicated that using a higher amount of Cr and V content increased the hardness of mild steel up to 876 HV. These findings and visual investigations suggest that the hardfacing electrode was applied successfully to all samples, and it formed similar structures regardless of the substrate material carbon ratio.

The performance of the hardfaced samples was also evaluated by ball-on-disc wear tests. Figure 4 shows the average wear area of samples. The wear behaviors of samples S1, S2, and S3, which were surface-alloyed with the PTA method, improved compared to the untreated samples. It was seen that this improvement becomes more dominant with the increase of the carbon ratio in the

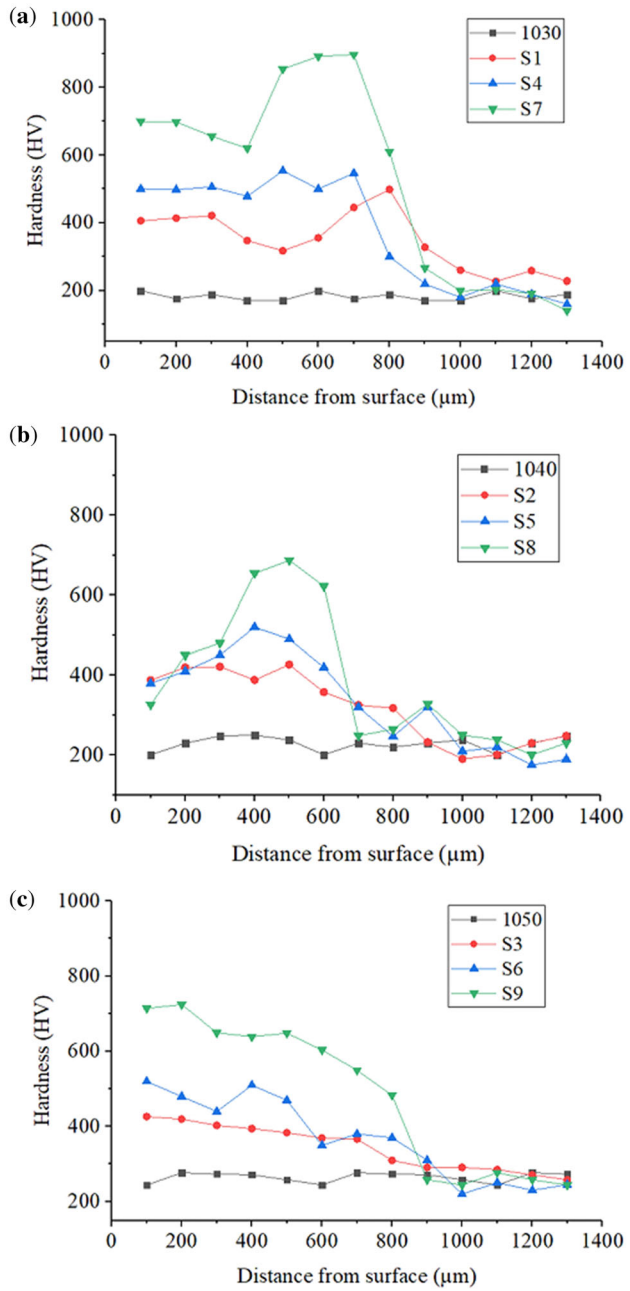

Figure 3. Microhardness distributions from surface to inside the parts for substrates (a) 1030, (b) 1040 and (c)1050.

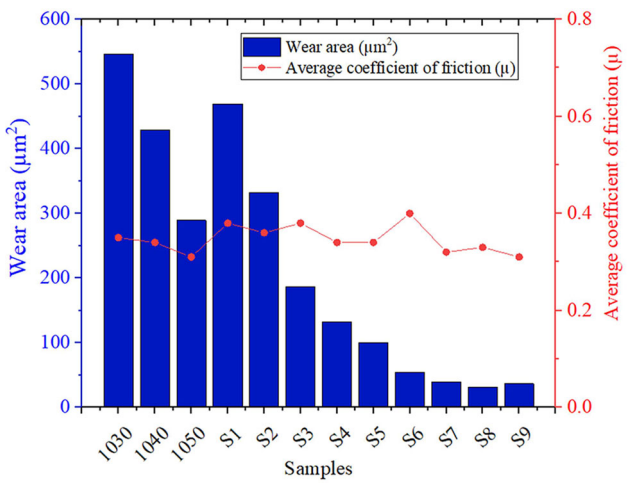

Figure 4. Average wear area of samples and the average coefficient of friction of samples.

substrate material. This can also be attributed to the formation of more carbides and borides and embedded hard particles that exist within the coating powder. The findings on the wear behavior of PTA-coated samples agree well with the literature. Ulutan *et al* [4] showed that PTA samples had lower weight loss than untreated samples, around 62.3 mg after 400 m of the abrasive test. Groups of S4, S6 samples were modified with Citodur 600 powder by using the SMAW method. The wear properties of these samples have improved compared to the untreated samples and PTA-treated group.

The other group, S7, S8, and S9 samples, were modified with "Toolcord" powder using the SMAWmethod. These samples were the most wear-resistant group among all test groups. Here, the resistance against plastic deformation of this group can be explained by the higher amount of carbide formation by the elements of W, V, and Cr elements found in the electrode. Based on all the results, it can also be said that the ratio of carbon content in the substrate material affects the success of the applied surface-alloying technique. According to the results of the wear test, significant wear resistance has been achieved with the operations made with Toolcord and Citodur 600 powders in plain carbon steels. In-situ friction coefficients of samples against WC ball were recorded during wear tests. Generally speaking, the friction coefficients were close to each other; the highest (COF) was obtained with the sample S6 ($\mu = 0.40$) while the lowest was recorded with 1050 ($\mu = 0.31$) (figure 4). The results were in concordance with the work of Ulutan *et al* [4] in which they found after PTA on AISI 4140 steel a COF value of 0.4.

3.2 *Corrosion results*

3.2a *Passivation behavior of coatings:* The passivation of a surface means the formation of oxide layers on the surface. Generally, a stable oxide layer is desired to control the corrosion. The formation of the oxide layer on the surface of the working electrode gives significant information about the corrosion resistance of the test sample. The anodic polarisation exhibited on samples 1030, S1, S4, and S7 were presented in figure 5. The Tafel values extracted from figure 5, E_{corr}, I_{corr}, β_a, and β_c values, were shown in table 4. When mild steels such as AISI 1030, AISI 1040, and AISI 1050 were subjected to the marine environment, compounds such as $FeCl_2$, $FeCl_2.4H_2O$, and $FeCl_3$. $6H_2O$ can be found on the surface of the working electrode besides iron oxides [15, 26]. Conversely, the addition of alloying element Cr between 0.3 and 0.4 wt.% can increase the corrosion resistance of mild steel in the marine environment [27]. Regarding the corrosion performance of the samples, lower corrosion potential was observed for sample S1 with −0.893 V, indicating better resistance to corrosion. In contrast, poor corrosion potential was observed for 1030 with −0.955 V. However, the untreated sample 1030

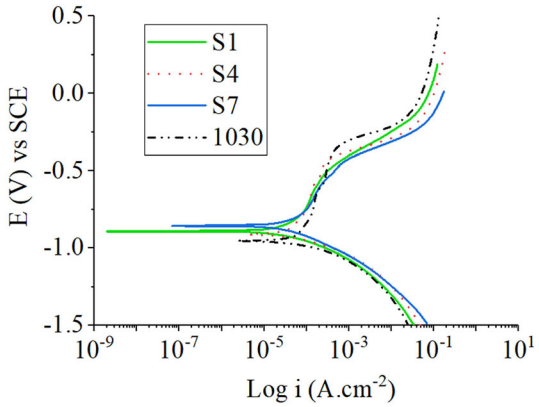

Figure 5. Anodic polarization plots of sample 1030, S1, S4, and S7 in the 3.5 wt.% NaCl solution.

showed a two-passivation zone in the region between −0.740 V and −0.41 V. This interval passivation can be an expression of the evolution of pitting and repassivation of pitting by corrosion products. On the other hand, the sample S4 had further similar passivation as 1030. It was located between −0.737 V and −0.469 V. Regarding the samples S1 and S7, the passivation zone was not apparent, but a decrease of corrosion current was observed when analyzing the slope between −0.740 V and −0.442 V. The lower corrosion rate was recorded for the sample S1 following by S7, S4, and 1030 (table 4). It can be stated here that sample S1 outperformed its rivals due probably to the presence of boron in the protective oxide film as boron oxide. The good influence of boron oxide powder on the corrosion of aluminum welds was also described in literature [28]. The S4 exhibited slightly poor corrosion resistance compared to S7 despite to higher content of Cr on the surface. However, the formation of two passivation zone (oxide layer) put in evidence the better corrosion resistance for S4 compared to S7.

The corrosion tests show that increasing the carbon content in the steel leads to a slight enhancement in the corrosion potential. It was also observed that a protective oxide film formed around −0.540 V and −0.400 V on sample 1040 (figure 6 and table 5).

Among the hard-faced samples, $SiC+B_4C$ coated sample S2 had lower corrosion potential with −0.901 V. Moreover, a similar passivation zone was noticed for S2 and S5, starting from −0.588 ending at −0.353 V. Here, the improved corrosion resistance of S5 can be explained by the higher quantity of Cr in the electrode that helps the resistance of oxide film. Bansod *et al* [19] also affirmed that using a higher amount of Cr in the electrode decreased the E_{corr} and I_{corr} values for SMAW and TIG. They registered an E_{corr} of −0.336 V and −0.327 V for SMAW and TIG-welded Cr-Mn stainless steel in 3.5% NaCl solution. For S8, two passivation regions were located; the first one around −0.775 V and −0.691 V, and the second one at

Table 4. The E_{corr}, I_{corr}, βa, and βc value calculated from the anodic plots in figure 5.

Sample	β_a (V/decade)	β_c (V/decade)	I_{corr} (μA)	E_{corr} (V)	Corrosion Rate (mpy)
1030	7.79E−01	1.00E−01	76.3	−0.955	34.01
S1	4.34E−01	1.23E−01	39.6	−0.893	18.10
S4	6.80E−01	9.59E−02	55.3	−0.911	25.29
S7	3.65E−01	1.45E−01	46.6	−0.858	21.27

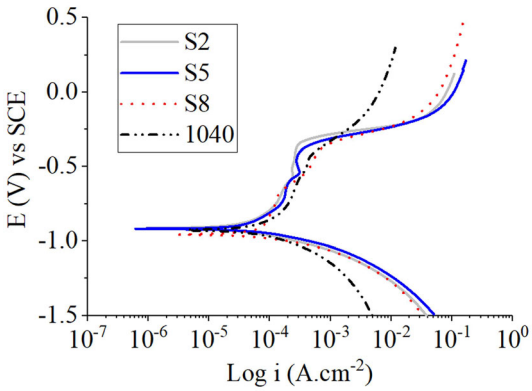

Figure 6. Anodic polarization plots of samples 1040, S2, S5, and S8 in the 3.5 wt.% NaCl solution.

Table 5. The E_{corr}, I_{corr}, βa, and βc value extracted from the anodic plots in figure 6.

Sample	β_a (V/decade)	β_c (V/decade)	I_{corr} (μA)	E_{corr} (V)	Corrosion Rate (mpy)
1040	1.36	2.50E−01	172	−0.927	76.76
S2	2.3E−01	2.47E−01	38	−0.901	17.56
S5	3.09E−01	6.85E−02	45	−0.918	20.58
S8	1.25E+00	8.02E−02	83	−0.956	37.00

−0.497 V and −0.401 V. This passivation at different intervals stemmed from the products formed after the pits corrosion. In the meantime, the lowest corrosion rate was recorded for S2, followed by S5, S8, and S1040.

Similar to the alloy 1030 and 1040, the anodic polarisation of 1050, which had the highest C amount, showed the lowest corrosion potential with −0.89 V compared to the coated materials S3, S6, and S9 (figure 7 and table 6). This poor performance of S3, S6, and S9 can be explained by the PTA and SMAW parameters such as voltage, current, etc. which influence largely the heat-affected zone and causing microstructure modification for hard coated 1050 compared to hardfaced 1030 and 1040. The better performance of 1050 compared to 1030 and 1040 was due principally to the higher content of the ferrite phase [31, 32]. On the other hand, poor corrosion potential was observed for sample S6. All samples displayed similar

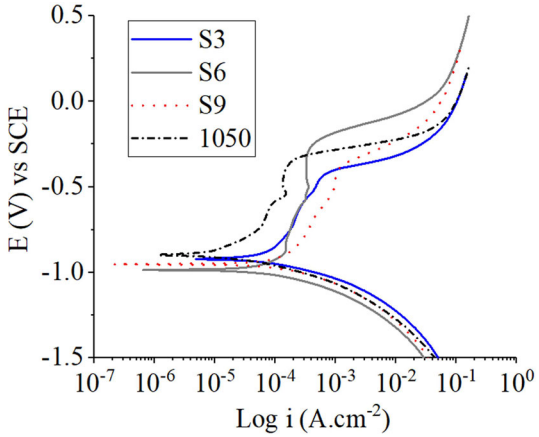

Figure 7. Anodic polarization plots of samples 1050, S3, S6, and S9 in the 3.5 wt.% NaCl solution.

passivation, but it was more pronounced for the sample S6, which exhibited the largest passivation zone: it began from −0.856 V and finalized −0.266 V. Regarding the corrosion rate, surprisingly, the uncoated 1050 had the lowest while the highest rate was obtained with S9.

3.2b *Corrosion resistance behavior of the coatings:* The EIS technique allows researchers to analyze the kinetic process between the surface (electrode) and solution (electrolyte). The Nyquist plots for samples 1030, S1, S4, and S7 were demonstrated in figure 8. In the marine environment, data for 1030 displayed a depressed semi-circle capacitive loop at high frequency and inductive loop at low frequency, pointing that the corrosion mechanism is followed by adsorption and desorption of species. When coating AISI1030 with Citodur 600, the resistance increased slightly at a higher rate and at a lower frequency for S4, while coating with Toolcord (sample S7) decreased the resistance. However, sample S1 exhibited a higher semi-circle with a lower adsorption process at low frequency. It should be noted that at low frequency, the inductive loop can be ascribed to the ion transfer [29, 30]. On the other hand, the S1 showing the largest loop, indicating that the sample had better passivation compared to rivals due to slow current transfer. Also, these findings validate the potentiodynamic results described above in samples 1030, S1, S4, and S7.

The effect of a slight increase of carbon in the mild steel was further investigated, and the results were presented in figure 9. At first glance, it can be seen that there exist a semi-circle loop and inductive loop situated at high frequency and at low frequency, such as in figure 8. The diameter of the semi-circle loop of S5 was higher than its rivals, which suggests that the oxide film was more protective. Conversely, poor resistance was observed for the sample AISI 1040.

When regarding the EIS resistance of the sample untreated and treated 1050, the EIS behavior was different

Table 6. The E_{corr}, I_{corr}, βa, and βc value extracted from the anodic plots in figure 7.

Sample	β_a (V/decade)	β_c (V/decade)	I_{corr} (μA)	E_{corr} (V)	Corrosion Rate (mpy)
1050	6.74E−01	1.58E−01	32.9	−0.897	15
S3	5.78E−01	1.02E-01	85.2	−0.921	39
S6	1.147	1.20E−01	116	−0.986	52
S9	6.10E−01	1.34E−01	167	−0.953	74

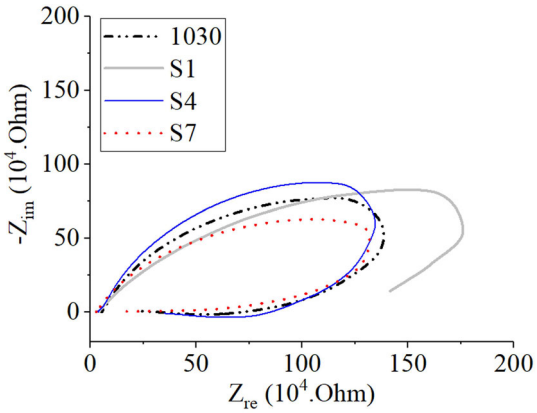

Figure 8. The Nyquist plot of the samples 1030, S1, S4, and S7 in the 3.5 wt.% NaCl solution.

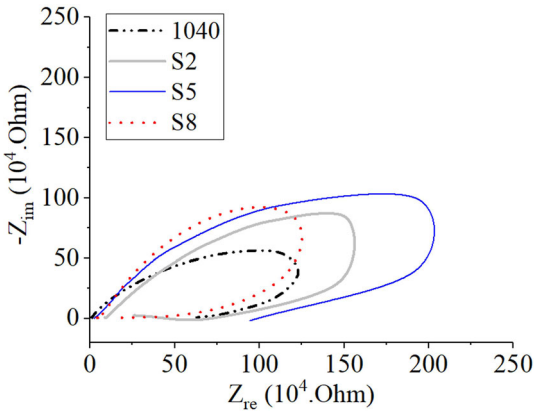

Figure 9. The Nyquist plot of the samples 1040, S2, S5, and S8 in the 3.5 wt.% NaCl solution.

compared to low carbon steel alloys. A higher capacitive loop or oxide layer formation was noticed for the alloy S6 compared to 1050, S3, and S9 (figure 10). On the other hand, the 1050 and S3 had marginally similar corrosion protection at high frequency. Moreover, the inductive loop was also observed, meaning the stabilization of layers by

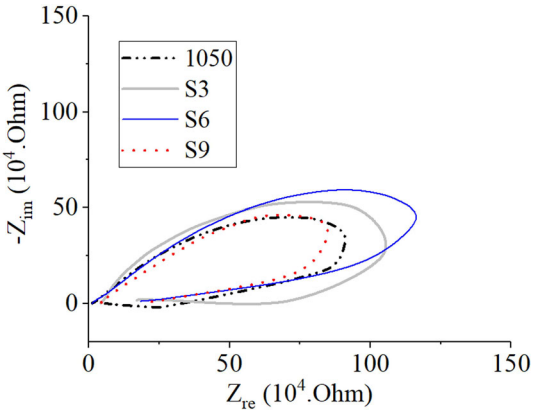

Figure 10. The Nyquist plot of the samples 1050, S3, S6, and S9 in the 3.5 wt.% NaCl solution.

corrosion products. In general, it can be stated here that all samples formed a protective layer, but it was more pronounced for S6, followed by S3, S9, and 1050.

4. Conclusion

According to the results of the experimental study, SiC + B_4C, Citodur 600, and Toolcord powders were successfully applied to AISI 1030, 1040, and 1050 plain carbon steels by using the PTA and SMAW methods. As a result of the surface alloying application, the surface hardness of the coated samples increased significantly, and the highest hardness of 896 HV was obtained with Toolcord powder. Regarding the wear behavior, it was found that the applied coating powders' composition was the main factor in determining the wear performance. Additionally, the increase in the carbon content of the substrate material was beneficial for wear resistance. On the other hand, SiC+B_4C using the PTA method had better corrosion potential, and corrosion rate compared to SMAW coated samples. The corrosion tests showed that all samples exhibited semi-circle at high frequency and an inductive loop at low frequency, suggesting that AISI 1030 when coated with SiC+B_4C, while for AISI 1040 and AISI 1050 with powder Citodur performed better corrosion resistance. It can be said that by applying the correct coating powder and method on plain carbon steel, the wear and corrosion performance can be improved significantly.

References

[1] Singh M, Majid M, Akhtar M A, Arora H and Chawla K 2017 Wear behaviour of smaw hardfaced mild steel and influence of dilution upon hardfacing properties. *Int. J. Mech. Eng. Technol.* 8(7): 1652–1661

[2] Scheid A and Oliveira A S C 2013 Analysis of PTA hardfacing with CoCrWC and CoCrMoSi alloys. *Soldagem & Inspeção* 18(4): 322–328
[3] Hosmani S S, Kuppusami P and Goyal R K 2014 An introduction to surface alloying of metals. Springer, New York
[4] Ulutan M, Celik O N, Gasan H and Er U 2010 Effect of different surface treatment methods on the friction and wear behavior of AISI 4140 steel. *J. Mater. Sci. Technol.* 26(3): 251–257
[5] Ulutan M, Yildirim M M, Buytoz S and Celik O N 2010 Microstructure and Wear Behavior of TIG Surface-Alloyed AISI 4140 Steel. *Tribol. Trans.* 54(1): 67–79
[6] Alsaran A 2002 Determination of tribological properties of ion-nitrided AISI 5140 steel. *Mater. Charact.* 49(2): 171–176
[7] Pouranvari M 2010 On the weldability of grey cast iron using nickel based filler metal. *Mater. Des.* 31(7): 3253–3258
[8] Bepari M M A and Shorowordi K M 2004 Effects of molybdenum and nickel additions on the structure and properties of carburized and hardened low carbon steels. *J. Mater. Process. Technol.* 155–156: 1972–1979
[9] Sadeghi A, Moloodi A, Golestanipour M and Mahdavi Shahri M 2017 An investigation of abrasive wear and corrosion behavior of surface repair of gray cast iron by SMAW. *J. Mater. Res. Technol.* 6(1): 90–95
[10] Ferozhkhan M, Duraiselvam M, Kumar K and Bharath R 2016 Plasma transferred arc welding of Stellite 6 Alloy on stainless steel for wear resistance. *Procedia Technol.* 25: 1305–1311
[11] Bohatch R G, Athayde J N, Siqueira J C M, D'Oliveira A S C M and Scheid A 2015 Influence of processing on the microstructure and properties of CoCrMoSi alloy PTA coatings. *Soldagem & Inspeção* 20(2): 219–227
[12] Yaedu A E and D'Oliveira A S C M 2005 Cobalt based alloy PTA hardfacing on different substrate steels. *Mater. Sci. Technol.* 21(4): 459–466
[13] Gür A K, Yildiz T, Kati N and Kaya S 2019 Microstructure and wear of FeCrC, SiC and B_4C coated AISI 430 stainless steel. *Mater. Test.* 61(2): 173–178
[14] Ulutan M, Kiliçay K, Çelik O N and Er Ü 2016 Microstructure and wear behaviour of plasma transferred arc (PTA)-deposited FeCrC composite coatings on AISI 5115 steel. *J. Mater. Process. Technol.* 236: 26–34
[15] Alcántara J, Fuente D, Chico B, Simancas J, Díaz I and Morcillo M 2017 Marine atmospheric corrosion of carbon steel: a review. *Materials* 10(4): 406
[16] Alcántara J, Chico B, Díaz I, de la Fuente D and Morcillo M 2015 Airborne chloride deposit and its effect on marine atmospheric corrosion of mild steel. *Corrosion Sci.* 97: 74–88
[17] Busari Y O, Ahmed I I and Shuaib-Babata Y L 2017 Effect of heat input on the mechanical and corrosion behaviour of SMAW mild steel. *J. Prod. Eng.* 220(2): 59–64
[18] Srinivasan P, Muthupandi V, Dietzel W and Sivan V 2006 An assessment of impact strength and corrosion behaviour of shielded metal arc welded dissimilar weldments between UNS 31803 and IS 2062 steels. *Mater. Des.* 27(3): 182–191
[19] Bansod A and Patil A 2017 Effect of welding processes on microstructure, mechanical properties, and corrosion behavior of low-nickel austenitic stainless steels. *Metallogr. Microstruct. Anal.* 6(4): 304–317
[20] Mohammed R, Reddy G M and Rao K S 2015 Microstructure and pitting corrosion of shielded metal arc welded high nitrogen stainless steel. *Defence Technol.* 11(3): 237–243
[21] Heider B, Oechsner M, Reisgen U, Ellermeier J, Engler T, Andersohn G, Sharma R, Gonzalez Olivares E and Zokoll E 2020 Corrosion resistance and microstructure of welded duplex stainless steel surface layers on gray cast iron. *J. Thermal Spray Technol.* 29(4): 825–842
[22] d'Oliveira A S, Vilar R and Feder C G 2002 High temperature behaviour of plasma transferred arc and laser Co-based alloy coatings. *Appl. Surf. Sci.* 201(1): 154–160
[23] Gür A, Cengiz M and Taşkaya S 2019 Mikroalaşımlı Hardox 400 Çelik Yüzeyinin Plazma Transferli Ark Kaynak Yöntemiyle Alaşımlandırılması ve İncelenmesi. *DÜMF Mühendislik Dergisi* 10(3): 969–979
[24] Santos A X, Maciel T M, Costa J D, Sousa M B, Prasad S, Campos A R N and Santana R A C 2019 Study on influence of the PTA-P welding process parameters on corrosion behavior of Inconel 625 coatings. *Matéria* 24(1): e-12282
[25] Çelik O N 2013 Microstructure and wear properties of WC particle reinforced composite coating on Ti6Al4V alloy produced by the plasma transferred arc method. *Appl. Surf. Sci.* 274: 334–340
[26] Cornell R M and Schwertmann U 2003 The Iron Oxides: Structure, Properties, Reactions, Occurrences and Uses. 2nd edn. Wiley-VCH Verlag GmbH; Weinheim, Germany
[27] Ahmad Z 2006 Principles of Corrosion Engineering and Corrosion Control. Butterworth-Heinemann, Oxford, pp 479–549
[28] Öteyaka M and Ayrtüre H 2015 A study on the corrosion behavior in sea water of welds aluminum alloy by shielded metal arc welding, friction stir welding and gas tungsten arc welding. *Int. J. Electrochem. Sci.* 10: 8549–8557
[29] Huang W H, Yen H W and Lee Y L 2019 Corrosion behavior and surface analysis of 690 MPa-grade offshore steels in chloride media. *J. Mater. Res. Technol.* 8(1): 1476–1485
[30] Maleeva M A, Rybkina A A, Marshakov A I and Elkin V V 2008 The effect of atomic hydrogen on the anodic dissolution of iron in a sulfate electrolyte studied with impedance spectroscopy. *Protection Metals* 44(6): 548–556
[31] Clover D, Kinsella B, Pejcic B and De Marco R 2005 The influence of microstructure on the corrosion rate of various carbon steels. *J. Appl. Electrochem.* 35(2): 139–149
[32] Mohd Fauzi M A, Saud S N, Hamzah E, Mamat M F and Ming L J 2019 In vitro microstructure, mechanical properties and corrosion behaviour of low, medium and high carbon steel under different heat treatments. *J. Bio- Tribo-Corrosion* 5(2): 37